JOURNAL OF GEOPHYSICAL RESEARCH, VOL. 100, NO. B7, PAGES 12,405–12,422, JULY 10, 1995

Tomography of the crust and upper mantle in southeast Europe

C.B. Papazachos,[1] P.M. Hatzidimitriou, D.G. Panagiotopoulos, and G.N. Tsokas

Geophysical Laboratory, Aristotle University of Thessaloniki, Thessaloniki, Greece

Abstract. Compressional velocity structure of the crust and the upper mantle in southeastern Europe (broader Aegean area) is studied by inverting residuals of the first *P* arrivals from earthquakes in this region (16°E-31°E, 34°N-43°N). The data used are from regional events recorded by the permanent network of stations during the period 1971-1987, enriched with data from experiments with portable seismographs in four regions of this broad area. This study confirms the strong variations of crustal thickness in this area as well as the subduction of the eastern Mediterranean lithosphere under the southern Aegean and gives further detailed information on the crustal and upper mantle structure of the area. Important new information is the existence of a low-velocity crustal layer in western Greece and Albania and that the velocity anomaly in the mantle under the southern Aegean extends much farther and deeper to the northeast than the Benioff zone of the intermediate depth earthquakes indicates. Furthermore, evidence is presented about the possible existence of older subduction in the northern Aegean and about the influence of the tectonic regime on the velocity field.

Introduction

The velocity structure of southeastern Europe exhibits great complexity [e.g., *Spakman et al.*, 1993]. This complexity results from the geodynamic evolution of this area which plays an important role in the formation of the presently observed tectonic structure. In fact, the velocity field is often used to image the tectonic regime (and therefore to test models of geological evolution) and vice versa [*De Jonge et al.*, 1993].

The dominant tectonic feature of this area (Figure 1) is the subduction of the African plate beneath the Eurasian plate along the Hellenic arc [*Papazachos and Comninakis*, 1969-1970, 1971; *Papazachos and Delibasis*, 1969; *McKenzie*, 1970, 1972, 1978; *Le Pichon and Angelier*, 1979; *Wortel et al.*, 1990]. As a result of this subduction, the Aegean exhibits the characteristic structure of a marginal sea, with volcanic activity [*Georgalas*, 1962], magnetic anomalies and positive isostatic anomalies [*Fleischer*, 1964; *Vogt and Higgs*, 1969; *Makris*, 1976], high heat flow [*Fytikas et al.*, 1985], and high attenuation of seismic energy [*Papazachos and Comninakis*, 1971; *Hashida et al.*, 1988]. The high shallow seismicity is expressed in reverse faults on the outer part and normal faults in the concave (inner) part of the Hellenic arc [*Comninakis*, 1975; *McKenzie*, 1978], while the intermediate depth seimicity has a well-defined Benioff zone [*Papazachos and Comninakis*, 1969-1970, 1971]. The westward motion of Turkey is also of major significance. This is expressed by the right-lateral motion of the North Anatolia Fault and its continuation in the northern Aegean together with the North Aegean Trough (Figure 1). Contours of average depth of 100 and 160 km intermediate depth earthquakes in the southern Aegean [*Papazachos*, 1990] are also shown in Figure 1.

The velocity structure of the crust and upper mantle in this area has been studied using travel times from local earthquakes [*Papazachos et al.*, 1966; *Panagiotopoulos and Papazachos*, 1985] or explosions [*Makris*, 1972, 1978; *Voulgaris*, 1991], dispersion of surface waves [*Papazachos et al.*, 1967; *Calganile et al.*, 1982], and gravity data [*Makris*, 1973; *Chailas et al.*, 1992]. A preliminary Moho map of the area based on all the previously published studies is presented in Figure 2 [*Papazachos*, 1993]. Strong variations of crustal thickness are observed. The crust is more than 40 km thick under the Dinarides-Hellinides mountain chain but is locally thinning to less than 25 km in the back arc area (Aegean Sea). This thinning, which is also confirmed by gravity studies [*Makris*, 1976; *Chailas et al.*, 1992; *Papazachos*, 1994], is mainly attributed to the back arc spreading of the Aegean Sea.

The first results from seismic tomography were presented only recently and allowed a more detailed description of the lithosphere and the mantle. These previous studies [*Spakman*, 1986, 1988; *Spakman et al.*, 1988, 1993; *Ligdas et al.*, 1990; *Ligdas and Main*, 1991] tried to establish the principal features of the lithosphere-upper mantle system, to a depth of 800 km or more. Other studies concentrated on more local scales [*Drakatos*, 1989; *Drakatos et al.*, 1988, 1989; *Martin*, 1988; *Christodoulou and Hatzfeld*, 1988; *Ligdas and Lees*, 1993]. The large-scale structure of the crust and uppermost mantle has not been studied in detail. In all the regional studies, the crust is treated as one layer [*Drakatos and Drakopoulos*, 1991; *Ligdas et al.*, 1990] or as a part of the first layer [*Spakman*, 1988]. Moreover, the number of stations and arrivals used is limited.

In the present work, more than 100,000 *P* arrivals from 4,229 earthquakes in the region 16°E-31°E and 34°N-43°N are used for the determination of the detailed structure of the

[1]Now at Department of Geological and Geophysical Sciences, Princeton University, Princeton, New Jersey.

Copyright 1995 by the American Geophysical Union.

Paper number 95JB00669.
0148-0227/95/95JB-00669$05.00

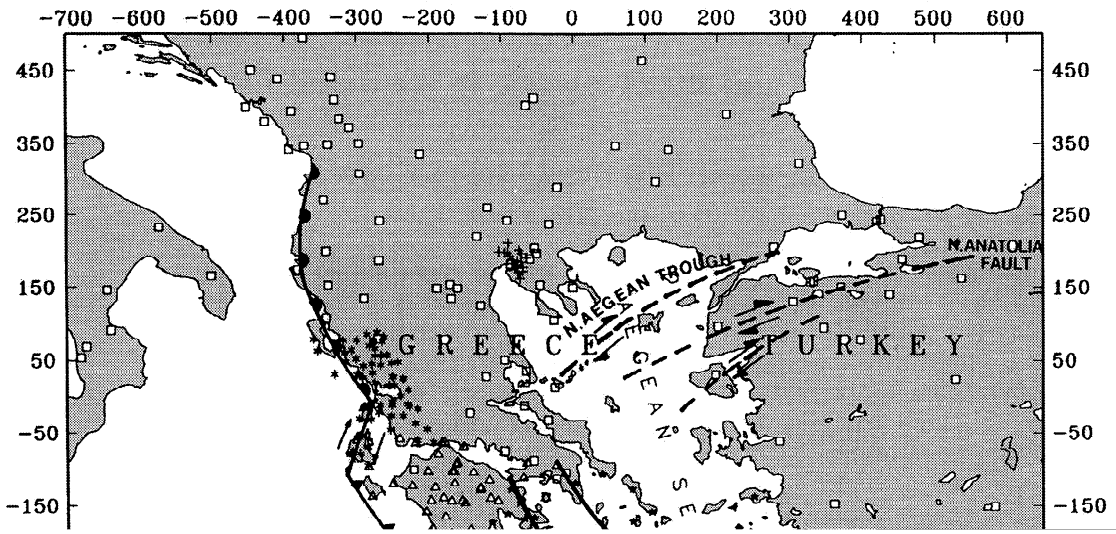

The data we used in this study come from the annual bulletins of the Geophysical Laboratory of the University of Thessaloniki (GLUT) for the time period 1981-1987 for events with surface wave magnitude $M_S \geq 3.5$. We added data from the International Seismological Center (ISC) bulletins, as relocated by *Karacostas* [1988], for the period 1971-1980 for events with surface wave magnitude $M_S \geq 5.0$. The original data come from the preliminary monthly bulletins of the National Observatory of Athens (NOA), GLUT, and seismological laboratories of neighboring countries (Italy, Albania, Yugoslavia, Bulgaria, and Turkey). The available travel times, parts of which were not routinely reported to ISC, were used in GLUT for the compilation of a new, more accurate epicentral map of the area, using a local model [*Panagiotopoulos and Papazachos*, 1985]. The data were enriched with observations from four local experiments (Figure 1) in the Thessaloniki basin (northern Greece), Peloponnesus (southern Greece), southern Aegean, and Epirus (northwestern Greece). These data were collected during the summers of 1985, 1986, 1988, and 1989, respect-

data set, quality criteria were established, involving the number of observations and the distance of the closest recording station from the epicenter of each event. The main

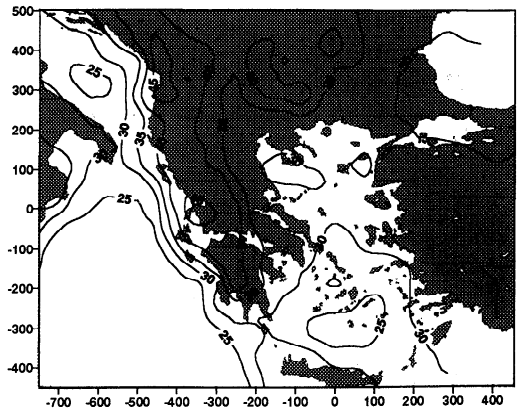

Figure 2. Preliminary map of the Moho discontinuity in southeastern Europe (modified from [*Papazachos*, 1993]).

target of this filtering process was to avoid using events with poorly constrained locations. No event with less than 10 P arrivals was used unless it was recorded by the local networks where a minimum number of 8 P phases was required. Moreover, for events recorded by the regional network, we required the nearest station to be within 50 km from the epicenter. If this criterion was not fulfiled, then the minimum number of recording stations was set to 15 or 20, if the closest recording station was within 100 km or 150 km from the epicenter, respectively. This filtering process resulted in a final data set of 4,229 events. Approximately 20% of them (775 events) were recorded by the temporary local networks. The final data set consisted of 109,655 P and 25,357 S arrivals recorded at 327 stations.

Travel times were further checked in order to assure that only first arrivals were used. The travel time-distance plot revealed that especially for the S arrivals, the P_g (S_g) branches extended to distances larger than the critical ($\simeq$150 km), since the first P_n (S_n) arrivals were missed in some cases. These extended (P_g and S_g) branches, as well as other outliers, were cut off by rejecting all travel times which had a residual larger than 6 s from the least squares linear fit to the P_g (S_g) and P_n (S_n) branches.

The final epicenters of the events for which data were used are shown in the map of Figure 3. The locations of the stations are depicted in Figure 1. In Figure 4, the frequency histogram of the P arrivals used for each earthquake is shown. It is observed that for the majority of the earthquakes, more than 14 arrivals were used.

Model Configuration and Inversion Method

In local inversion studies, a flat Earth layered model is commonly used [*Aki and Lee*, 1976]. However, as the scale of the survey increases, the errors due to the spherical shape of the earth cannot be neglected. In our case, the dimensions of the study area were approximately 1200 km X 1000 km, and therefore the Earth's curvature needs to be taken into account. However, we would still like to use a "cartesian" system of coordinates for convenience (as in a flat Earth model). In the present study, we adopted the Tranverse Mercator Projection (TMP) which establishes a curvilinear cartesian system on the Earth's surface. If we choose the center of our coordinate system in the center of our area, then the maximum angular error of the TMP is less than 0.4° and the maximum distance error is around 0.4%. However, the distance error was calculated for each ray and travel times were corrected accordingly. Using this coordinate system, we created a three-dimensional (3-D) grid of cells of equal size with constant velocity. The horizontal dimensions of each cell were 100 km X 100 km.

Following Roecker's [1981] modification of the *Aki and Lee* [1976] method, the travel time residual for a given ray is a function (in a first-order approximation) of the corrections to the hypocenter parameters and the velocities of the cells hit by the ray. The whole data set forms a linear system of equations $\Delta\mathbf{T} = \mathbf{A}\,\Delta\mathbf{X} + \mathbf{B}\,\Delta\mathbf{V}$. The hypocenter matrix of this equation, **A**, can be separated [*Pavlis and Booker*, 1980] from the slowness matrix, **B**, resulting in a linear system of the form:

$$\Delta\boldsymbol{T}' = \boldsymbol{B}'\,\Delta\boldsymbol{V} \tag{1}$$

where $\Delta\mathbf{T}'$ and $\Delta\mathbf{V}$ are the altered residual and velocity correction vectors and $\mathbf{B}'$ is the altered velocity derivative matrix.

For the ray tracing, we incorporated the approximate ray tracing scheme of *Thurber and Ellsworth* [1980]. In this approach, an equivalent one-dimensional (1-D) structure is calculated from the three-dimensional model for the epicenter station path. The direct and refracted waves are calculated in this "equivalent" model, and the fastest ray is selected after the travel time is recalculated in the three-dimensional medium. The main disadvantage of this kind of approximate ray tracing is that the spatial mapping of the velocity anomalies is not always quite accurate, since the implied ray

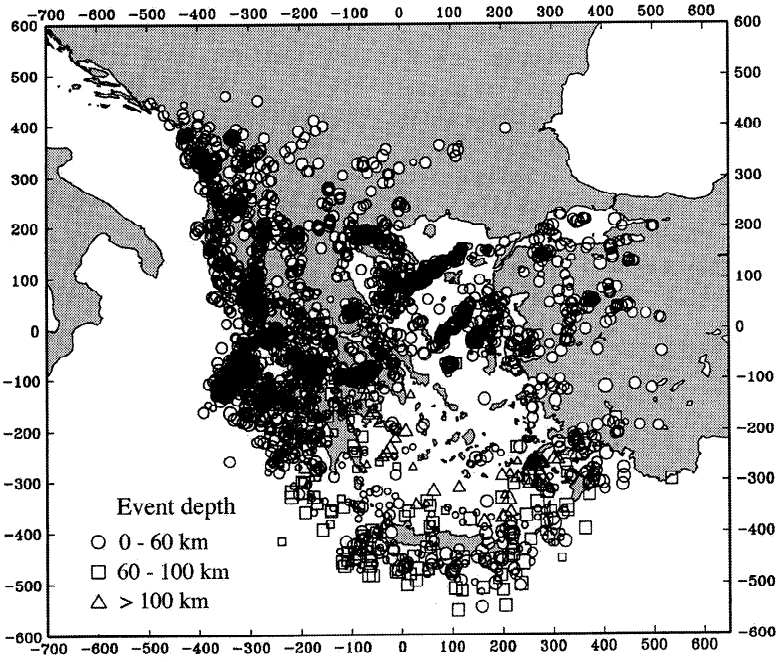

Figure 3. Map of the finally determined epicenters of the events for which data were used in this study. The events have been separated into three groups according to their focal depth.

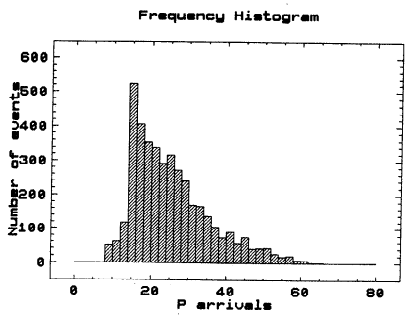

Figure 4. Frequency histogram of the P arrivals used for each event in the present study.

geometry is very simple (direct or refracted rays, ray lies on the vertical plane connecting hypocenter to station, etc.).

In order to perform the ray tracing in a spherical earth, some modifications need to be made in the geometry of the refracted and direct waves. The plots of direct and refracted ray paths used in this study are shown in Figure 5. For the refracted waves, the travel time for an event at depth h (Figure 5a) is similar to the flat Earth case:

$$T = \frac{r_p \Delta}{r_0} + \sum_{i=1}^{p-1} \frac{(V_P^2 - a_i^2 V_i^2)^{\frac{1}{2}}}{V_P\, V_i} z_i +$$

$$+ \sum_{i=k}^{p-1} \frac{(V_P^2 - a_i^2 V_i^2)^{\frac{1}{2}}}{V_P\, V_i} z_i - \frac{(V_P^2 - a_K^2 V_K^2)^{\frac{1}{2}}}{V_P\, V_K} h_K \qquad (2)$$

where $a_i = r_p / r_i'$, r_p is the radius of the top of the p layer, and r_i' is the average radius of the i layer. For the direct waves, the false position and secant method are used, adapted for a spherical Earth.

In the present work, the linear system (1) was solved using the damped least squares method [*Levenberg*, 1944; *Marquadt*, 1966; *Franklin*, 1970] where a damping coefficient, ε^2, is added to the diagonal of the normal equations matrix. Resolution and errors were formally calculated using singular value decomposition (SVD) [*Lanczos*, 1961]. Various damping factors were tried in order to evaluate the trade-off between resolution and error. From this analysis the value of $\varepsilon^2 = 300$ s^4/km^2 was selected for the final solution. The effect of large residuals was smoothed out by applying an exponential decaying weight of the form $1/[1+a \exp(b^*\text{res})]$ to residuals larger than 3 s. After the calculation of the velocity structure, the events were relocated in this new structure. This procedure was repeated in an iterative scheme. At each step, the velocity model was computed for a second grid which had half a grid offset in both horizontal dimensions with respect to the original one, and the final velocity structure resulted as the average of the two.

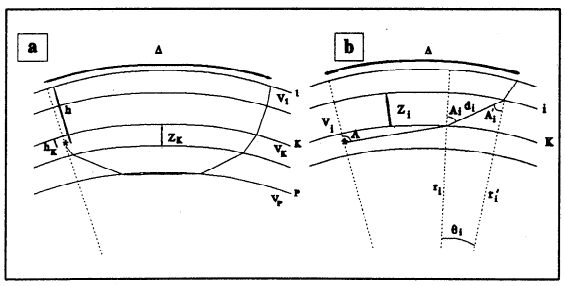

Figure 5. Geometry of the (a) refracted and (b) direct waves used in the present study.

Inversion of the Data

Initially, a one-dimensional model was calculated by treating each layer as a single cell. Both P and S velocities were calculated for each layer and are presented in Table 1. The crust (maximum thickness $\simeq$ 40 km) was divided into four layers with a thickness of 10 km. The upper mantle was divided into layers of increasing thickness with depth. However, these discontinuities are not entirely insignificant. The 20 km and 30 km depth layer boundaries approximately correspond to the bottom of the "granitic" (19 km) and the "basaltic" (31 km) layers for the average model of the area [*Panagiotopoulos and Papazachos*, 1985]. The 40 km depth is about equal to the maximum crustal thickness in the area. The last one (160 km) is near the maximum depth of the intermediate depth events in the southern Aegean Benioff zone [*Papazachos and Comninakis*, 1971].

Only P velocity structure was calculated from the inversion. Unfortunately, since less than 15% of the stations had three-component seismometers, the S arrivals data set is relatively unreliable. However, the S arrivals were used in the event relocation, since their constraint on the hypocenters was necessary. Large S residuals were also weighted in a similar way with the P residuals. The S velocity structure used in these calculations was derived from the P velocities using the corresponding V_P/V_S ratios for each layer, as these were derived from the 1-D model.

After some trial runs, we elected to include all cells with more than 25 hits in the inversion. In Figures 6a-6h the cell hit maps for the eight layers of our model are presented, where we observe a good coverage up to the depth of 90 km. The sampled space decreases rapidly in the last two layers since only rays from intermediate depth events hit these layers. The cell hit density in the upper layers is mainly controlled by the distribution of the recording stations. This results in local areas of relatively poor coverage, especially in the first two layers (0-20 km), like the northeastern part of the study area (eastern Bulgaria-European part of Turkey).

Table 1. One-Dimensional Velocity Model Used in the Three-Dimensional Inversion

Depth, km	P Velocity, km/s	S Velocity, km/s
0-10	5.96	3.30
10-20	6.09	3.33
20-30	6.74	3.76
30-40	7.31	3.96
40-60	7.77	4.41
60-90	7.97	4.58
90-120	8.10	4.66
120-160	8.12	4.68
160-	8.20	4.70

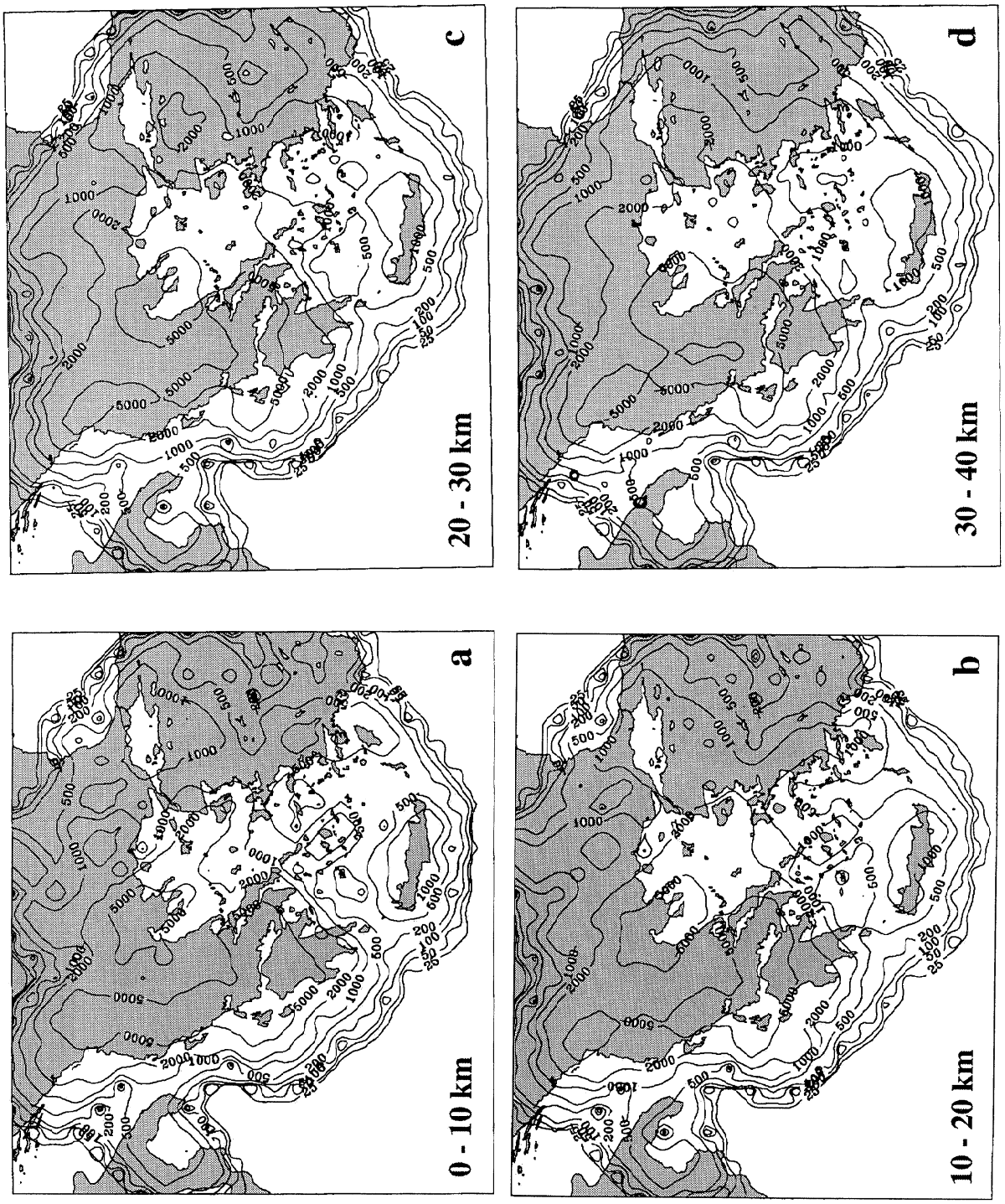

Figure 6. (a-h) Distribution of the density of seismic rays (number of cell hits) within each layer. Depth range is indicated in the figures.

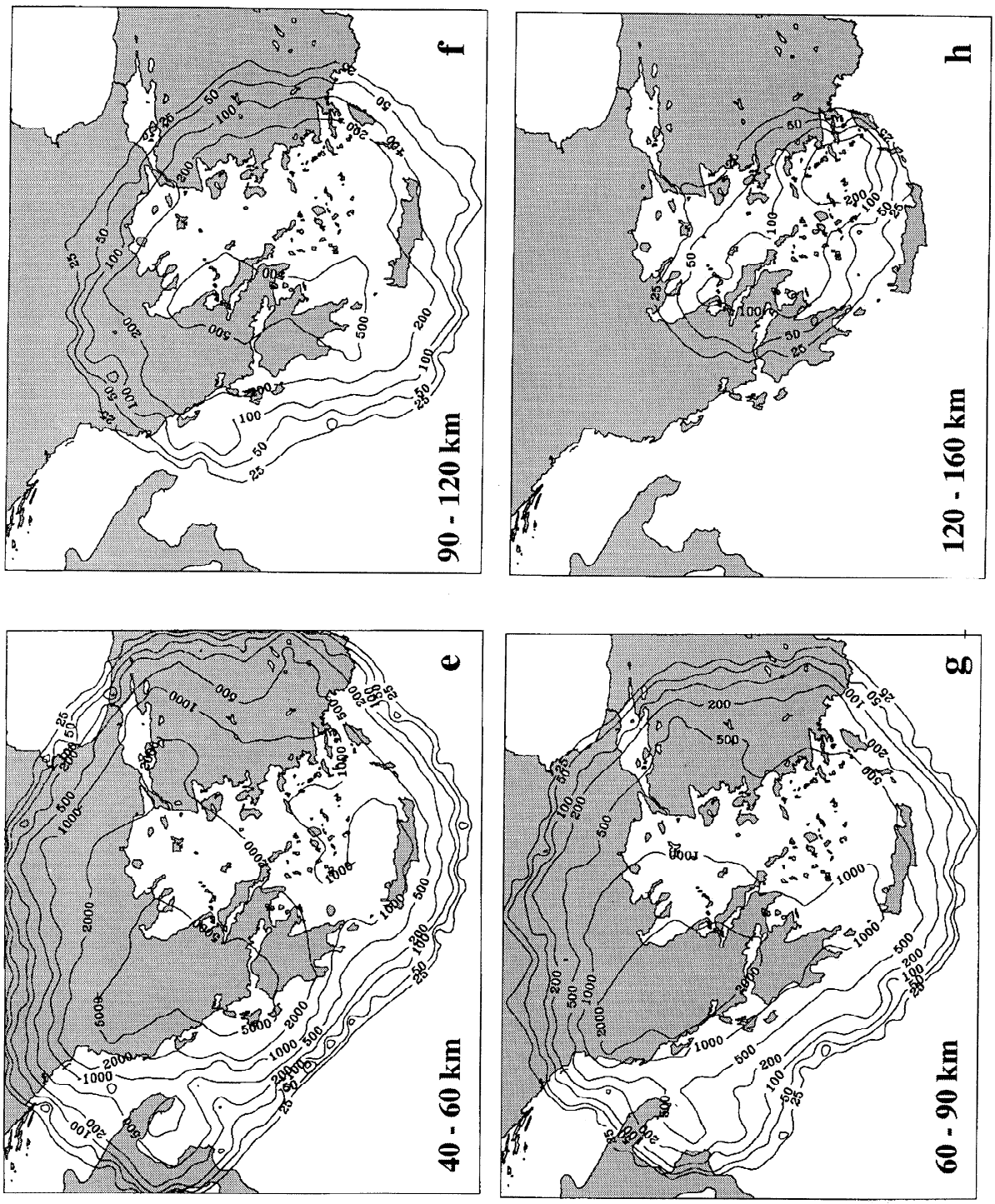

Figure 6. (continued)

Starting from this one-dimensional model, we iteratively calculated the final three-dimensional model. Further variance reduction was negligible after four iterations. The final rms improvement (raw residuals) was 36.7% (23.0%, 11.8%, 4.7%, and 2.1% for the four iterations, respectively) and the final rms was 0.83 s. At each iteration, all events were relocated in the new model. The average total horizontal change was 4.8 km and the average total vertical change was 2.9 $\pm$ 7.6 km. Very few foci changed more than 20 km in either horizontal or vertical direction. The average change in the origin time was -0.50 $\pm$ 1.11 s and in almost all cases was between -3.5 s and 2 s. The frequency histogram of the final standard deviations (Figure 7) is a superposition of two histograms, one for the regional events, recorded by the permanent stations, and one for the events of the local experiments, recorded by portable stations, with average values around 0.9 s and 0.3 s, respectively.

If we compare the epicenters finally determined (Figure 3) with the initial ones, we cannot detect any obvious changes, horizontal or vertical, for the surface events. However, for the intermediate depth events with hypocentral depths larger than 100 km, significant changes are observed. The number of events available did not allow a full three-dimensional reconstruction of the dipping Benioff zone. Instead, we plotted these events (Figure 8) against their distance from the already published contour of average focal depth equal to 100 km [*Papazachos*, 1990, Figure 1], before (Figure 8a) and after (Figure 8b) their relocation in the 3-D medium. In the outer (convex) part of the arc, we do not expect events with depths >100 km, as observed in Figure 8a, since the subduction takes place further to the north. In Figure 8b the intermediate depth seismicity is nicely relocated at depths not exceeding 100 km in the outer arc area. Moreover, Figure 8b suggests that the thickness of the African lithosphere (at least of the seismicaly active part) is around 90 km in this area. This hypocentral improvement strengthens the importance of the relocation in a three-dimensional medium, especially in a subduction zone, where strong velocity changes are observed.

Tomographic Images

In Figures 9a to 9h the velocity distribution within each layer is shown. In the first layer (Figure 9a), which corresponds roughly to the sedimentary and the upper crustal layer, the Aegean and Asia Minor generally exhibit low

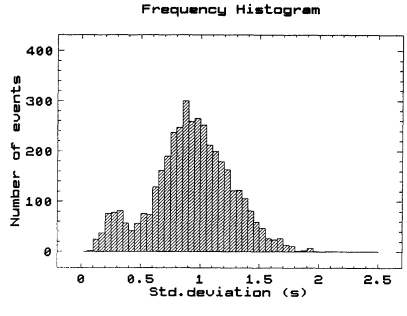

Figure 7. Frequency histogram of the final standard deviations of each shock for which data were used in the present study. A superposition of the histograms for the permanent and portable stations is observed, with average deviations around 0.9 and 0.3 s, respectively.

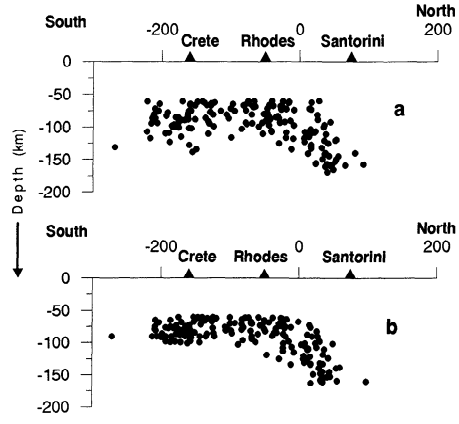

Figure 8. Plot of the intermediate depth events (h >60 km) of the present study using (a) the original and (b) the final (after the relocation) hypocenters.

velocities (5.2-5.8 km/s). Northern Greece shows high velocities within a zone of northwest-southeast direction where velocities above 6.2 km/s are detected. This zone almost coincides with the geologic Servomacedonian zone, consisting of metamorphic formations. The Dinarides-Hellenides mountain chain (southern Yugoslavia, Albania, Epirus, Peloponnesus, Cre-te, Rhodes, southwestern Turkey), which will be referred to as DHMC hereinafter, shows typical upper crust velocities (5.9-6.1 km/s). However, a low-velocity anomaly is observed in the western part of Albania and Epirus (northwestern Greece). This anomaly seems to dip to the east and appears to extend along the DHMC in the second layer (Figure 9b). In the inner part of the Aegean typical upper (6.0-6.2 km/s) and lower (6.5-6.7 km/s) crustal velocities are observed.

In the third layer (Figure 9c), the velocities along the DHMC are around 6.1-6.3 km/s, showing that we are still in the upper crust. However, in the southern Aegean we have lower crust velocities (6.5-6.7 km/s), as a result of the crustal thinning [e.g., *Makris*, 1973] in the volcanic arc above the south Aegean Benioff zone. This effect is also pronounced in the northern Aegean, along and to the north of the North Aegean Trough, where even higher velocities are observed. The sharp southern boundary of this high-velocity zone coincides with the southern edge of the North Aegean Trough (Figure 1), which trends in a similar northeast-southwest direction. Although, the existence and extent of the crustal thinning in this area have been a matter of debate [*Brooks and Kiriakidis*, 1986], it seems that the crust is thinner in this area than in the southern Aegean. These last two observations suggest a possible connection of the North Aegean Trough with deeper tectonic phenomena.

The fourth layer (Figure 9d) exhibits higher velocity contrasts. This is due to the fact that along the DHMC (up to Crete), the crust is around 35-40 km thick (or more). Therefore the velocities in this area are typical of the crust just above Moho (6.5-6.9 km/s). However, in the northern Aegean (along and to the north of the North Aegean Trough), southern Aegean, Asia Minor, and southern Adriatic, the crust is thinner ($\leq$30 km, Figure 2). As a result, for this layer, the velocities in these areas are much higher (7.5-7.9 km/s), representing the upper mantle. These relatively low sub-Moho velocities (around 7.8 km/s) are characteristic for this area [*Papazachos et al.*, 1966].

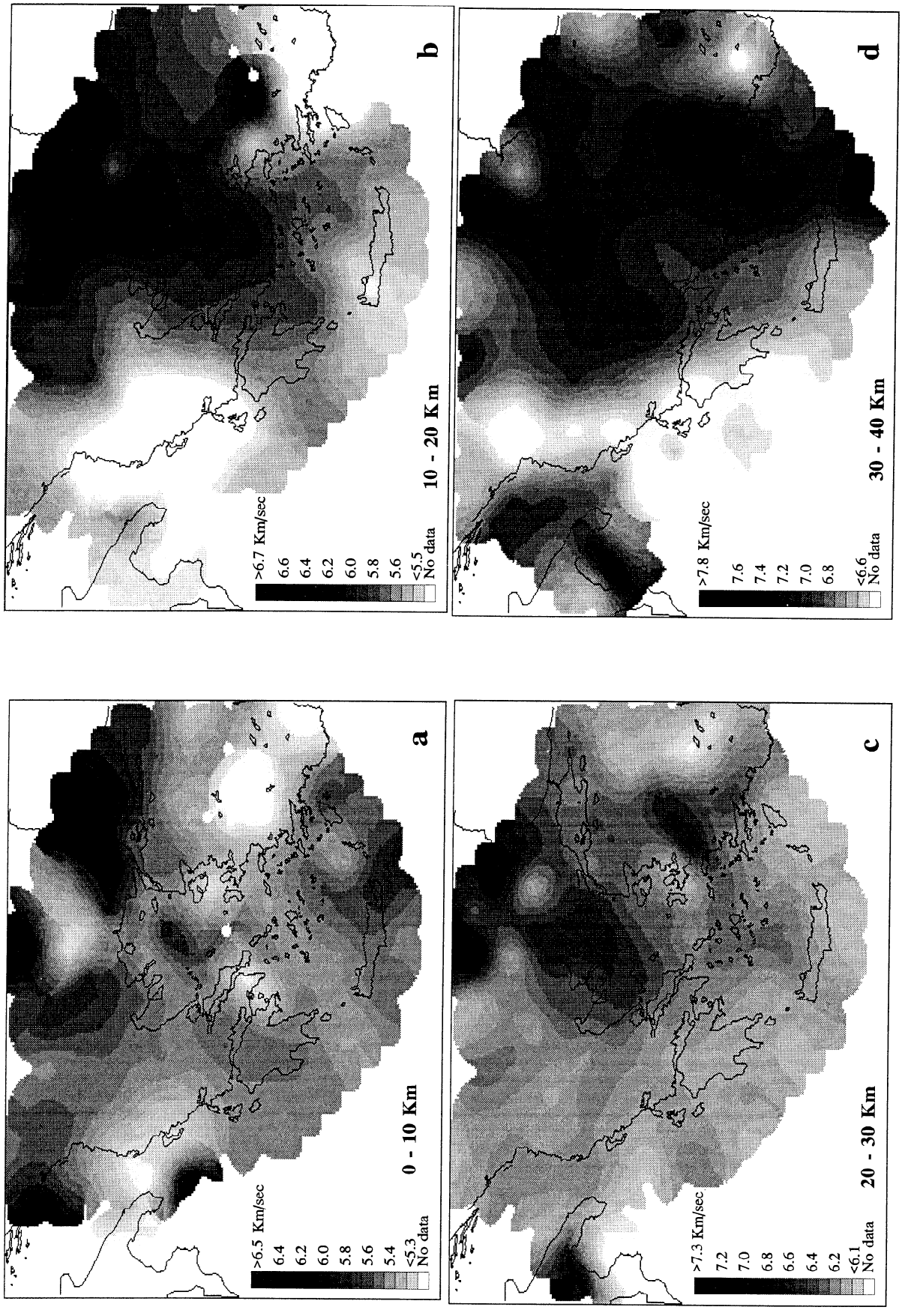

Figure 9. (a-h) Tomographic images of the crust and upper mantle in southeastern Europe in 16-level gray scale. Depth range is indicated in the figures.

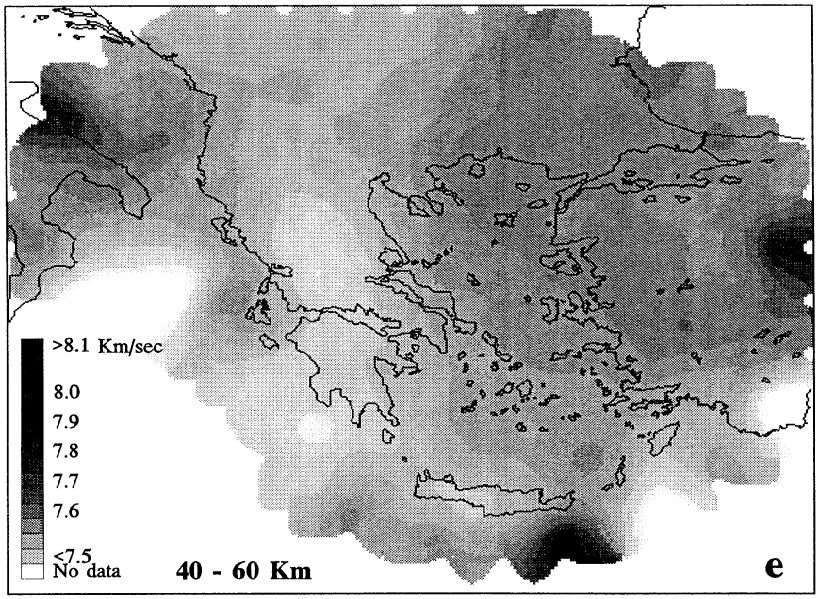

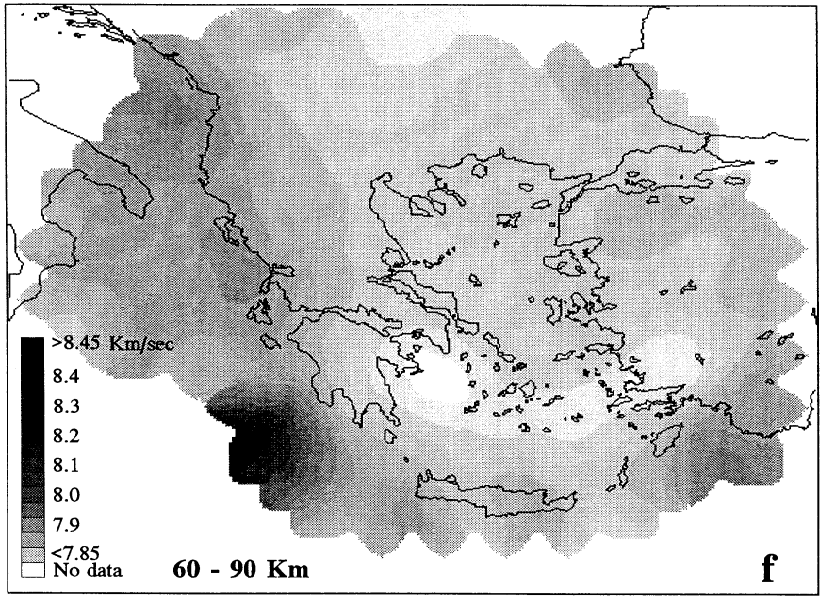

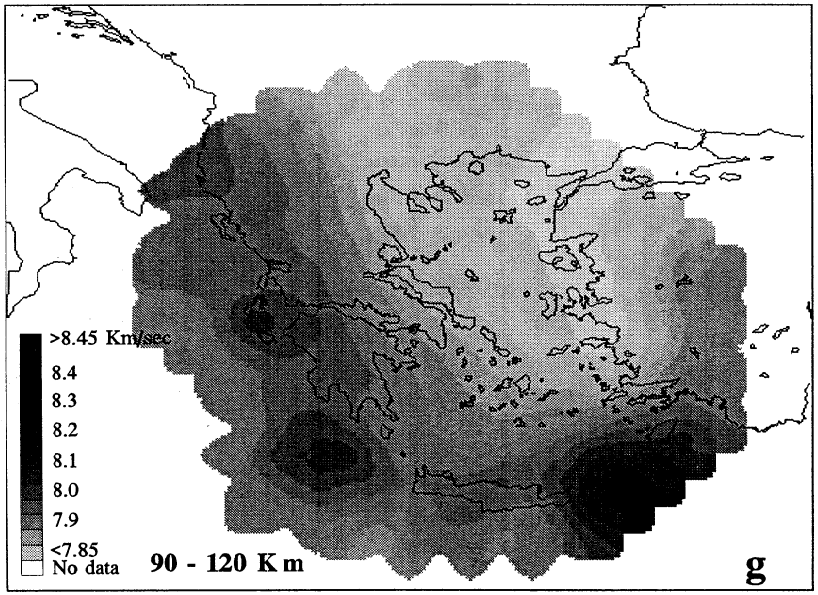

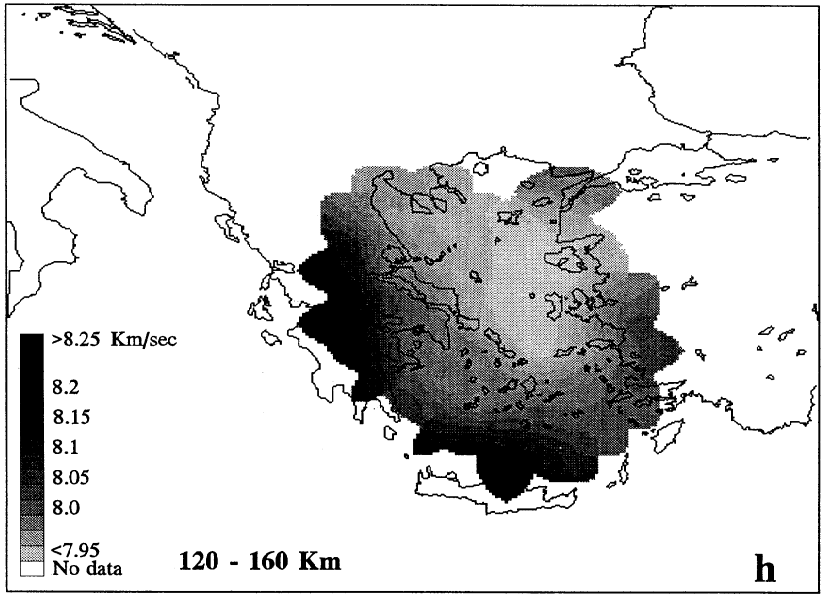

Figure 9. (continued)

The fifth layer (Figure 9e) shows upper mantle velocities in all its extent. Along the DHMC, where the overlying crust is thick, relatively low velocities, around 7.6 km/s, are observed. This image is completely changed in the next layer (60-90 km, Figure 9f). The velocity structure is now controlled by the subduction process in the southern Aegean and not by crustal thickness variations. Along the outer Hellenic arc, a high-velocity zone appears, corresponding to the dipping African lithosphere. This zone extends further to the north, along the western part of Epirus, Albania, and southern Yugoslavia. In the inner part of the Hellenic arc, a low-velocity zone is observed, just below the volcanic arc. The amphitheatrical shape of this zone coincides very well with the shape of the dipping lithosphere. This suggests that the low velocities in this area are simply a result of the high heat flow due to partial melting above the underlying subducting lithosphere (see also the depth contours of the intermediate depth events in Figure 1).

This image is continued in the next layer (Figure 9g). Both the high-velocity (outer) and the low-velocity (inner) zones move further to the inner part of the Hellenic arc. The outer limits of the subducting lithosphere are starting to show as relatively low-velocity areas in the outer edges of the high-velocity zone. In the inner part of the arc, the low-velocity zone covers the whole Aegean sea and extends even further to the northeast (northern Greece, northwestern Turkey). This development of the velocity anomalies is almost identical in the last layer (120-160 km, Figure 9h), although its spatial extent is not resolved because of the lack of seismic rays which penetrate it.

Some velocity anomalies, especially at the edges of all tomographic images, can sometimes be ficticious and misleading. This is due to the fact that the peripheral cells are not well sampled by seismic rays. A typical example is the anomalies in the first four layers (Figure 9a-9d) in the northeastern edge of the picture (eastern coasts of Bulgaria-European part of Turkey). In this region both the earthquake distribution and the station coverage are quite sparse. This results in an almost uniform velocity (6.3-6.8 km/s) for these first four crustal layers.

In Figures 10a-10h and 11a-11h the distribution of the diagonal elements of the resolution and error matrices is shown. The presentation is made in a way so that areas with large errors and poor resolution have lighter shading. Both resolution and errors exhibit a similar distribution. In the first two layers (0-20 km), where the distribution of seismic rays is very inhomogeneous (Figure 6a-6b), relatively large errors ($\geq$0.2 km/s) and medium- to low-resolution values (0.4-0.8) are observed in the eastern Aegean and Asia Minor. Therefore interpretation of velocity anomalies in these areas, especially when their spatial extent is limited, should be made with great care. In the next two layers (20-40 km), only $\simeq$10% of the cells exhibit resolution values below 0.7 and errors $\geq$0.25 km/s (Figure 10a-10b and 11a-11b). In the upper mantle ($\simeq$40-160 km), the images are well resolved (only 4% of the cells have errors >0.1 km/s and resolution <0.7), as a result of the dense and homogeneous distribution of seismic rays (Figure 9e-9g). In the last layer the situation is slightly different, since a limited number of rays are reaching these depths.

Discussion and Conclusions

The present study confirms that the P wave velocity structure of the crust and upper mantle in southeastern Europe shows strong horizontal variations as a result of the complicated crustal structure and the subduction process in the southern Aegean.

The velocity distribution in the shallow layers presented in the present study (0-10 km, 10-20 km, 20-30 km, 30-40 km, 40-60 km) is strongly influenced by the variation of the depth of the Moho discontinuities. Of special interest is the identification of a low-velocity layer (LVL) at a depth between about 10 and 20 km in western Greece and Albania. The spatial extent of this LVL can be seen in Figure 12 where the differences of the velocities of the first two layers are shown. Dark shaded areas exhibit lower velocities in the second layer (10-20 km) than the overlying one (0-10 km) and therefore define the LVL at the depth of 10-20 km. It is quite clear that this LVL is practically limited under the DHMC. The higher velocity contrast, which locally exceeds 0.5 km/s, is observed under Albania and western Greece. The errors in the velocities of the 0-10 km and 10-20 km layers in this area are smaller than 0.1 km/s and 0.15 km/s, respectively. Therefore these errors could not account for the observation of this LVL. The existence of the LVL under this area (thicker crust-higher mountain chain) shows a possible connection with the Alpidic orogenesis. Similar crustal LVLs at these depths have been reported for many other mountain chains like the Swiss Alps (Swiss geotraverse [*Buchi and Trumphy*, 1976]) or Rhinegraben [*Prodehl et al.*, 1976]. The interpretation of this LVL is not straightforward. A connection seems to exist between the LVL and areas of crustal thickening and vertical uplift like mountain chains. *Landisman et al.* [1971] and *Mueller* [1977] suggest that the LVL is created due to granitic or other intrusions in the crust during this uplift, as directly observed in some cases [*Labhart*, 1975]. On the other hand, deep drilling and seismic exploration by the Greek Public Petroleum Co. [*Monopolis and Bruneton*, 1971; *G.Marnelis*, personal communication 1993] have revealed the existence of thick (locally up to 5-6 km) Triassic formations in the Ionian geological zone (western coasts of Albania and Greece). These evaporites are dipping toward the northeast (like the low-velocity anomaly in Figure 9a) under the inner geological zones (Gavrovo, Pindos), that is, under the Hellinides mountain chain. At the same time, they exhibit significantly lower velocities (5.2-5.6 km/s) than the overlying formations (5.9-6.2 km/s), and therefore they could account for the existence of the LVL under the DHMC.

The velocity structure of the deeper layers (60-160 km) reveals the subduction process in the southern Aegean. The African lithosphere appears as a high-velocity dipping zone, having an amphitheatrical shape in the southern Aegean. In Figure 13 the velocity distribution along two profiles in the western and eastern part of the south Aegean Benioff zone is presented. Both profiles are approximately normal to the 100 km average depth contour. A higher dipping angle, around 25°, is observed in the eastern part of the arc in comparison to the 10° of the western arc. These values are in agreement with the observed increase of the dipping angle of the Benioff zone from west to east [*Papazachos and Comninakis*, 1971].

A low-velocity area appears in the inner part above the subducting lithophere. This area, as well as the high-velocity zone representing the subducting lithosphere, extend much further to the northeast than the present subduction, as this subduction is indicated by the intermediate depth events. This probably supports current ideas that the subduction has

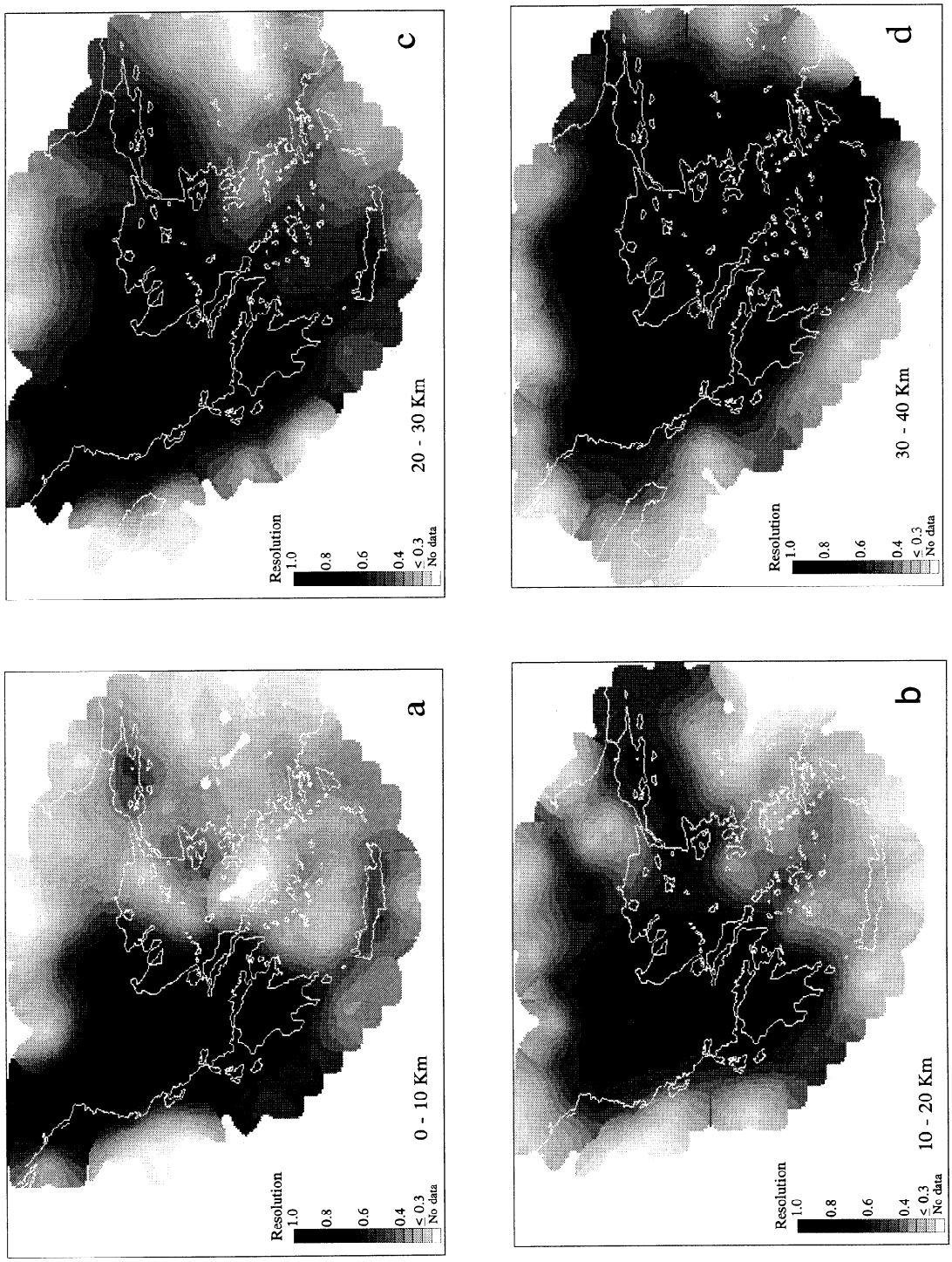

Figure 10. (a-h) Distribution of the diagonal elements of the resolution matrix within each layer in 16-level gray scale. Depth range is indicated in the figures.

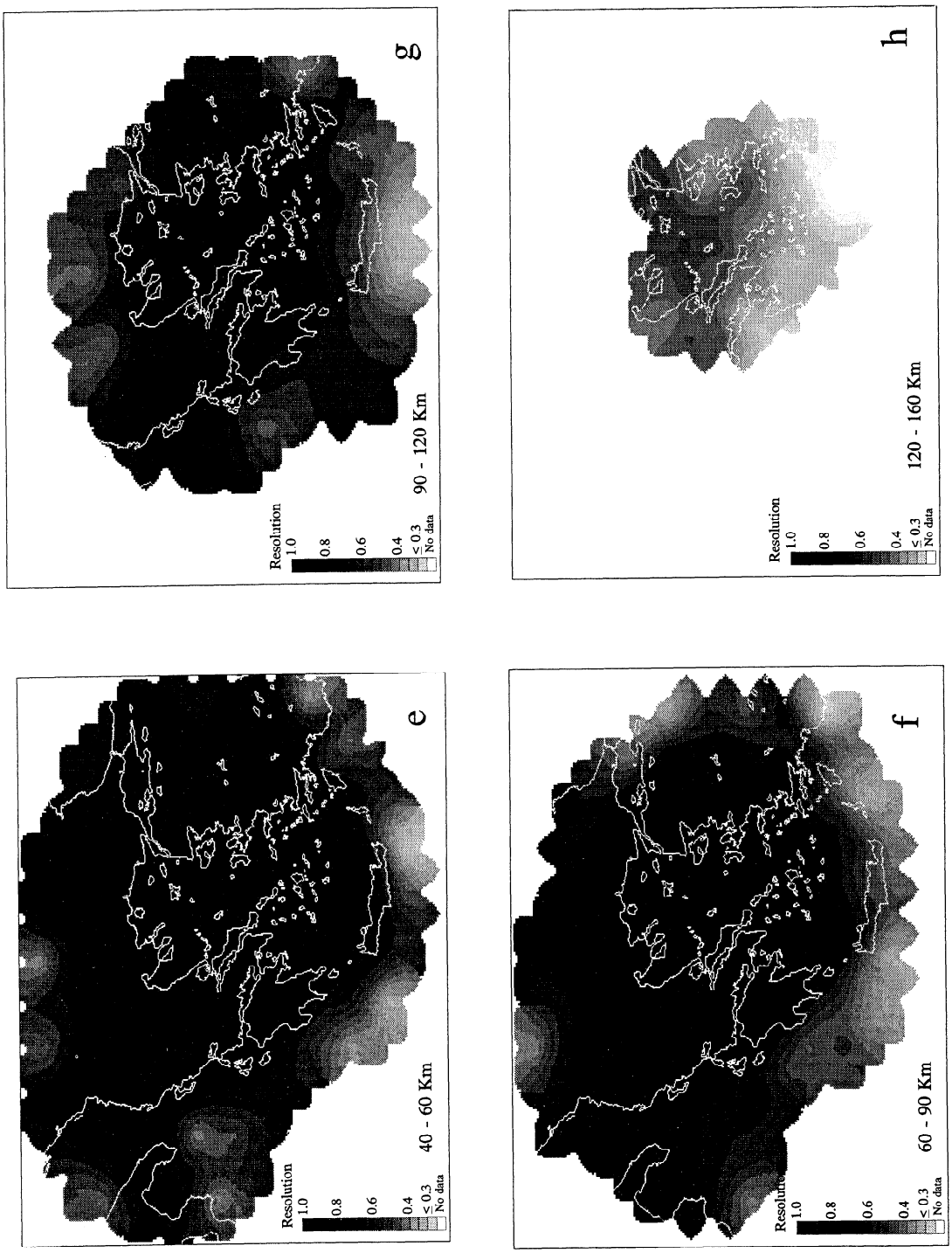

Figure 10. (continued)

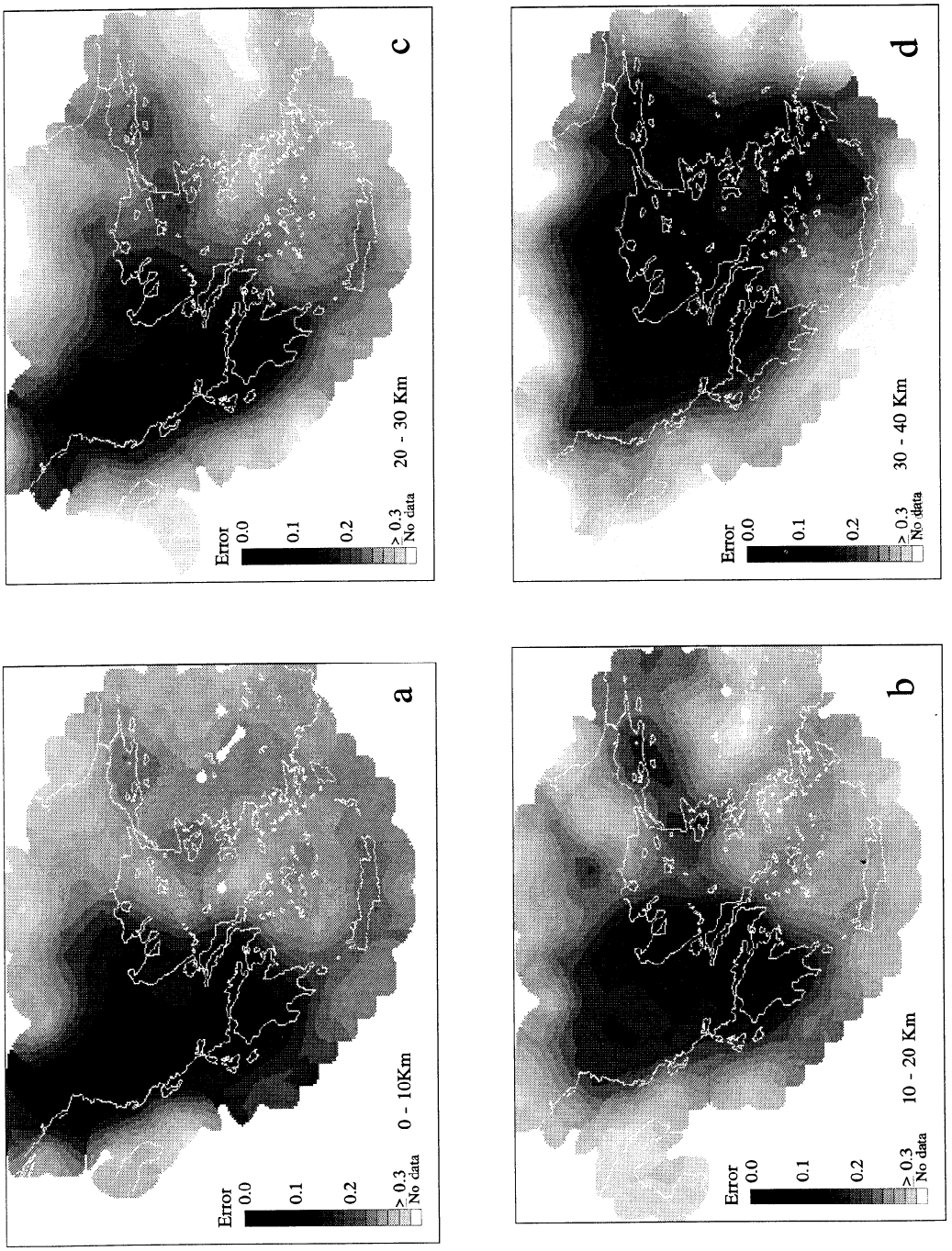

Figure 11. (a-h) Distribution of the diagonal elements of the error (square root of covariance) matrix within each layer in 16-level gray scale. Depth range is indicated in the figures.

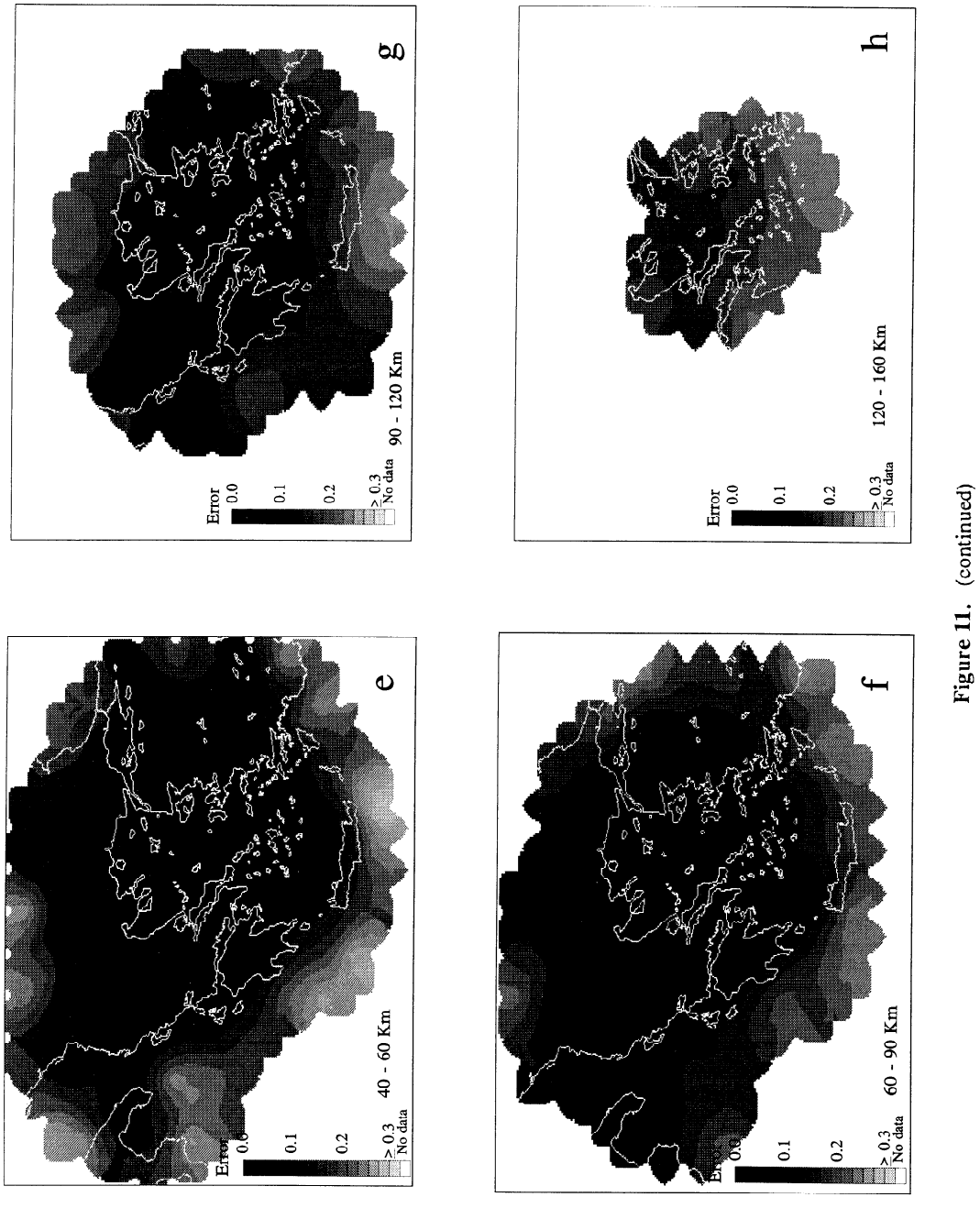

Figure 11. (continued)

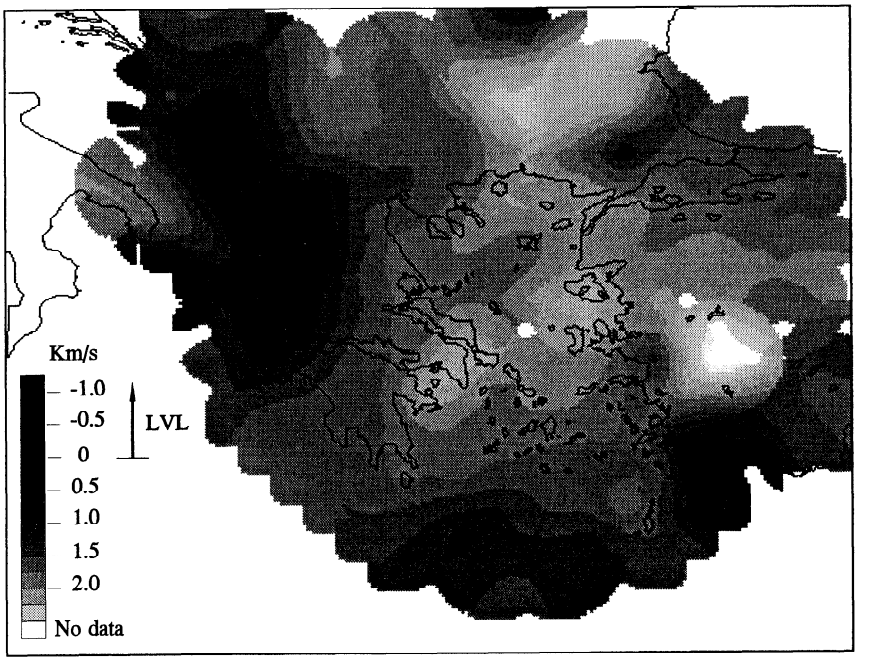

Figure 12. Map of the velocity contrast between the first (0-10 km) and the second (10-20 km) layers. Heavily shaded areas (negative values) define the limits of the crustal low-velocity layer (LVL) at depths around 10-20 km.

gradually migrated from the northern Aegean to its present position, possibly since Eocene [*De Jonge et al.*, 1993], leaving the velocity anomalies as a trace of its migration. Some observations [*Shanov et al.*, 1992] indicate the possible existence of an old subduction in the northern Aegean. This old subduction is also suggested by Figure 14 where the velocity distribution at the depth of 90-120 km after the third iteration is presented. An area of low velocities is observed, trending parallel to the North Aegean Trough (see Figure 1), resulting in a geophysical image similar to the southern Aegean. However, this low-velocity anomaly is not very well resolved and it is not present in the final results (Figure 9f). Although the rms improvement in the last iteration was only ~2%, we cannot rule out that the shape and position of this anomaly are an artifact.

An important feature of the tomographic images is the lineament of the velocity contrasts within each layer. In the first four layers (0-40 km), all the lineament have an east-west to east/northeast-west/southwest direction in Asia Minor which changes to northeast-southwest in the Aegean. The trending of this lineament is parallel to the direction of the North Aegean Trough and the continuation of the strike-slip

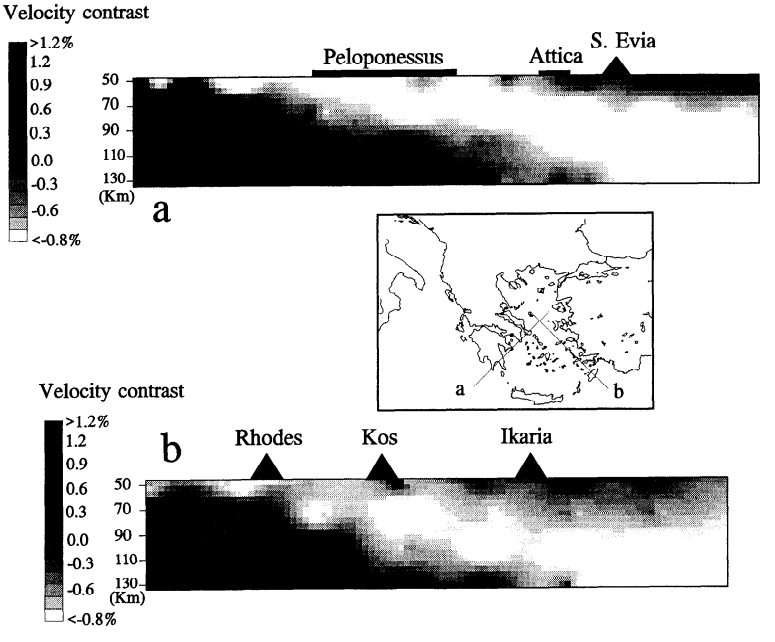

Figure 13. Velocity distribution along two profiles in the (a) western and (b) eastern parts of the Hellenic arc. Both profiles are almost normal to the 100 km average depth contour of the south Aegean Benioff zone.

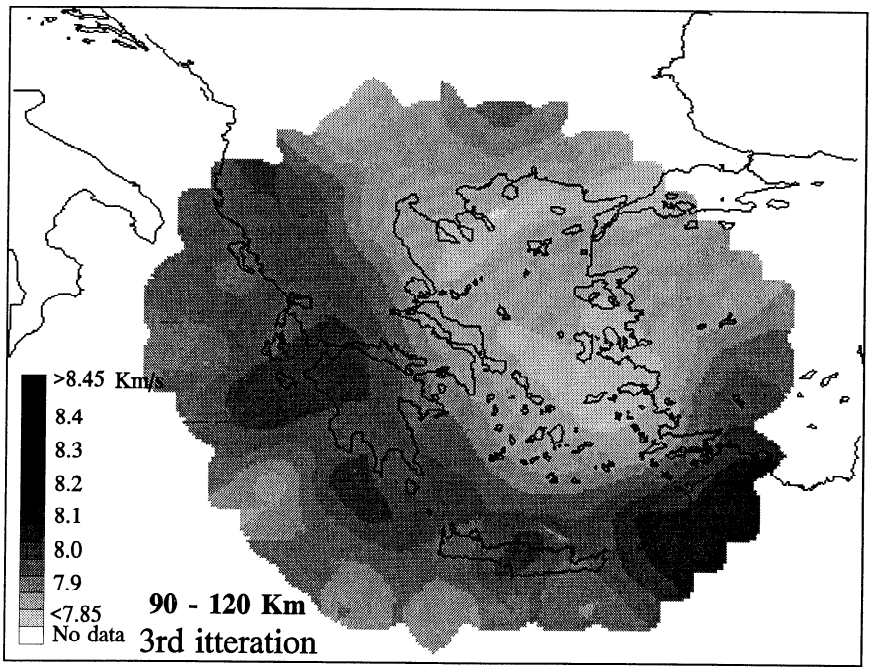

Figure 14. Velocity distribution at the depth of 90-120 km after the third iteration of the inversion.

North Anatolia Fault in the northern Aegean, as well as to the direction of the normal faults in the broader Aegean back arc area [*Papazachos et al.*, 1992]. This similarity suggests that the stress field and the resulting tectonic regime is directly reflected in the velocity distribution. This image is completely changed in the deeper layers, especially below 60 km, where the tomographic images are affected by the subduction of the African lithosphere.

Acknowledgments. We would like to thank D. Hatzfeld, B. Karakostas, E. Scordilis, and C. Papaioannou for providing part of the data and S. Roecker for the computer program which was used as a basis for the development of the new program used in this study. We are also gratefull to B. C. Papazachos for his careful reading of the manuscript, and his valuable suggestions. D. E. James, J. Luetgert and an anonymous reviewer are thanked for their detailed and critical review, and their useful suggestions. Part of this research was supported by the Greek Earthquake Protection and Planning Organization (research project 8513/93) and by the EC Environment Research Programs (contracts EV.5V-CT93-0281 and EV.5V-CT93-0285, Climatology and Natural Hazards).

References

Aki, K., and W. H. K. Lee, Determination of three-dimensional velocity anomalies under a seismic array using first *P* arrival times from local earthquakes, 1, A homogeneous initial model, *J. Geophys. Res., 81,* 4381-4399, 1976.

Brooks, M., and L. Kiriakidis, Subsidence of the North Aegean Trough: An alternative view, *J. Geol. Soc. London, 143*, 23-27, 1986.

Buchi, U.P., and R. Trumphy, Bemerkungen zum geologischen Profillangs der Geotraverse Basel-Chiasso, *Schweiz. Mineral. Petrogr. Mitt., 56*, 589-603, 1976.

Calganile, G., F. D'Ingeo, P. Farrugia, and G. F. Panza, The lithosphere in the central-eastern Mediterranean area, *Pure Appl. Geophys., 120*, 389-406, 1982.

Chailas, S., R. G. Hipkin, and E. Lagios, Isostatic studies in the Hellenides, paper presented at the 6th Congress of the Geological Society of Greece, Geol. Soc. of Greece, Athens, Greece, May 25-27, 1992.

Christodoulou, A., and D. Hatzfeld, Three-dimensional crustal and upper mantle structure beneath Chalkidiki (northern Greece), *Earth Planet. Sci. Lett., 88*, 153-168, 1988.

Comninakis, P. E., A contribution to the investigation of the seismicity of the area of Greece (in Greek), Ph.D. thesis, 110 pp., Univ. of Athens, Athens, Greece, 1975.

De Jonge, M. R., M. J. R. Wortel, and W. Spakman, From tectonic reconstruction to upper mantle model: An application to the Alpine-Mediterranean region, *Tectonophysics, 223*, 53-65, 1993.

Drakatos, G., Seismic tomography - Determination of high and low velocity zones beneath Greece and surrounding regions. Ph.D. thesis, 144 pp., Univ. of Athens, Athens, Greece, 1989.

Drakatos, G., and J. Drakopoulos, 3-D velocity structure beneath the crust and upper mantle of the Aegean sea region, *Pure Appl. Geophys., 135*, 401-420, 1991.

Drakatos, G., J. Latoussakis, G. Stavrakakis, D. Papanastassiou, J. Drakopoulos, and A. Bourboulis, Examination of a velocity model using 3-D velocity structure technique, paper presented at the Workshop on Induced Seismicity and Associated Phenomena, Czech. Acad. of Sci., Liblice, Czechoslovakia, 1988.

Drakatos, G., J. Latoussakis, G. Stavrakakis, D. Papanastasiou, and J.Drakopoulos, 3-Dimensional velocity structure of the north-central Greece from inversion of travel times, paper presented at the 3rd Congress of the Geological Society of Greece, Geol. Soc. of Greece, Athens, 1989.

Fleischer, U., Schwerestorungen im ostlichen Mittelmeer: nach Messungen mit einem Askania-Seegravimeter., *Dtsch. Hydrogr. Z., 17*(4), 1964.

Franklin, J.N., Well-posed stochastic extension of ill-posed linear problems., *J. Math. Anal. Appl., 31*, 682-716, 1970.

Fytikas, M., F. Innocenti, P. Manetti, R. Mazzuoli, A. Peccerillo, and L. Villari, Tertiary to Quaternary evolution of the volcanism in the Aegean region, in *The Geological Evolution of the Eastern Mediterranean*, edited by J. E. Dixon, and A.

H. F. Robertson, pp. , Geol. Soc. Spec. Publ. 17, London, 1985.

Georgalas, G., *Catalogue of the Active Volcanoes and Solfatara Fields in Greece*, Part12, International Association of Volcanology, Rome, 1962.

Hashida, T., G. Stavrakakis, and K. Shimazaki, three-dimensional seismic attenuation structure beneath the Aegean region and its tectonic implication, *Tectonophysics, 145*, 43-54, 1988.

Hatzfeld, D., G. Pedotti, P. Hatzidimitriou, and K. Makropoulos, The strain pattern in western Hellenic arc, deduced from a microearthquake survey, *Geophys. J. Int., 101*, 181-202, 1990.

Hatzfeld, D., M. Besnard, K. Makropoulos, N. Voulgaris, V. Kouskouna, P. Hatzidimitriou, D. Panagiotopoulos, G. Karakaisis, A. Deschamps, and H. Lyon-Caen, Subcrustal microearthquake seismicity and fault plane solutions beneath the Hellenic arc, *J. Geophys. Res., 98*, 2861-2870, 1993.

Hatzidimitriou, P., D. Hatzfeld, E. Scordilis, and E. Papadimitriou, Seismotectonic evidence of an active normal fault beneath Thessaloniki, *Terra Nova, 3*, 648-654, 1992.

Karacostas, B., Relation between the seismic activity and geological and geomorphological features of the Aegean and surrounding area (in Greek), Ph.D. thesis, 243 pp., Univ. of Thessaloniki, Thessaloniki, Greece, 1994.

Labhart, T. P., *Geologie-Einfuhrung in die Erdwissenschaften*, 108pp., Hallwag, Bern, Switzerland, 1975.

Lanczos, C., *Linear Differential Operators*, Van Nostrand Reinhold, New York, 1961.

Landisman, M., S. Mueller, and B. J. Mitchel, Review of evidence for velocity inversions in the continental crust, in *The Structure and Physical Properties of the Earth's Crust*, Geophys. Monogr. Ser., Vol. 14, edited by J. G. Heacock, pp. 11-34, AGU, Washington, D.C., 1971.

Le Pichon, X., and J. Angelier, The Hellenic arc and trench system: A key to the neotectonic evolution of the eastern Mediterranean area, *Tectonophysics, 60*, 1-42, 1979.

Levenberg, K., A method for the solution of certain non-linear problems in least squares, *Q. Appl. Math., 2*, 164-168, 1944.

Ligdas, C. N., and J. M. Lees, Seismic velocity constrains in the Thessaloniki and Chalkidiki areas (northern Greece) from a 3-D tomographic study, *Tectonophysics, 228*, 97-121, 1993.

Ligdas, C. N., and J. G. Main, On the resolving power of tomographic images in the Aegean area, *Geophys. J. Int., 107*, 197-203, 1991.

Ligdas, C. N., I. G. Main, and R. D. Adams, 3-D structure of the lithosphere in the Aegean sea region, *Geophys. J. Int., 102*, 219-229, 1990.

Makris, J., Gravity and magnetic measurments on Peloponessus, Attica and Kithera and their preliminary interpretation, paper presented at the 23rd Congr. Ass. Plen. de la CIESM, CIESM, Athens, 1972.

Makris, J., Some geophysical aspects of the evolution of the Hellenides, *Delt. Hell. Geol. Hetair., 10*, 206-213, 1973.

Makris, J., A dynamic model of the Hellenic arc deduced from geophysical data, *Tectonophysics, 36*, 339-346, 1976.

Makris, J., The crust and upper mantle of the Aegean region from deep seismic soundings, *Tectonophysics, 46*, 269-284, 1978.

Marquadt, D. W., An algorithm for least squares estimation of non-linear parameters, J. Soc. Ind. Appl. Math., 11, 431-441, 1966.

Martin, C., Geometrie et cinematique de la subduction Egeenne structure en vitesse et en attenuation sous le Peloponnese (in French), Ph.D. Thesis, 261 pp., Universite Joseph Fourier, Grenoble, France, 1988.

McKenzie, D. P., The plate tectonics of the Mediterranean region, *Nature, 226*, 239-243, 1970.

McKenzie, D. P., Active tectonics of the Mediterranean region, *Geophys. J. R. Astr. Soc., 30*, 109-185, 1972.

McKenzie, D. P., Active tectonics of the Alpine-Himalayan belt: the Aegean sea and surrounding regions, *Geophys. J. R. Astr. Soc., 55*, 217-254, 1978.

Monopolis, D., and A. Bruneton, Ionian sea (western Greece): Its structural outline deduced from drilling and geophysical data, *Tectonophysics, 83*, 227-242, 1971.

Mueller, S., A new model of the continental crust, in *The Earth's Crust: Its Nature and Physical Properties*, Geophys. Monogr. Ser., Vol. 20, edited by J. G. Heacock, pp. 289-317, AGU, Washington, D.C., 1977.

Panagiotopoulos, D. G., and B. C. Papazachos, Travel times of Pn-waves in the Aegean and surrounding area, *Geophys. J. R. Astr. Soc., 80*, 165-176, 1985.

Papazachos, B. C., Seismicity of the Aegean and the surround ing area, *Tectonophysics, 178*, 287-308, 1990.

Papazachos, B. C., and P. E. Comninakis, Geophysical features of the Greek Islands Arc and Eastern Mediterranean Ridge, *C. R. Seances Conf. Reunie Madrid, 16*, 74-75, 1969-1970.

Papazachos, B. C., and P. E. Comninakis, Geophysical and tectonic features of the Aegean arc, *J. Geophys. Res., 76*, 8517-8533, 1971.

Papazachos, B. C., and N. D. Delibasis, Tectonic stress field and seismic faulting in the area of Greece, *Tectonophysics, 7*, 231-255, 1969.

Papazachos, B. C., P. Comninakis, and J. Drakopoulos, Preliminary results of an investigation of crustal structure in southeastern Europe, *Bull. Seismol. Soc. Am., 56*, 1241-1268, 1966.

Papazachos, B. C., M. Polatou, and N. Mandalos, Dispersion of surface waves recorded in Athens, *Pure Appl. Geophys., 67*, 95-106, 1967.

Papazachos B. C., A. A. Kiratzi, and E. E. Papadimitriou, Orientation of active faulting in the Aegean and surrounding area, paper presented at the 6th Congress of the Geological Society of Greece, Geol. Soc. of Greece, Athens, Greece, May 25-27, 1992.

Papazachos, C. B., Determination of crustal thickness by inversion of travel times with an application in the Aegean area, paper presented at the 2nd Congress of the Greek Geophysical Union, Greek Geophys. Union, Florina, Greece, May 5-7, 1993.

Papazachos, C. B., Structure of the crust and upper mantle in SE Europe by inversion of seismic and gravimetric data (in Greek,. Ph.D Thesis, 208 pp., Univ. of Thessaloniki, Thessaloniki, Greece, 1994.

Pavlis, G. and J. Booker, The mixed discrete-continuous inverse problem: Application to the simultaneous determination of earthquake hypocenters and velocity structure, *J. Geophys. Res., 85*, 4801-4810, 1980.

Prodehl, C., J. Ansorge, J. B. Edel, D. Emter, K. Fuchs, S. Mueller, and E. Peterschmitt, Explosion-seismology research in central and southern Rhine Graben - A case history, in *Explosion Seismology in Central Europe*, edited by P. Giese, C. Prodehl, and A. Stein, pp. 313-328, Springer-Verlag, New York, 1976.

Roecker, S. W., Seismicity and tectonics of the Pamir-Hindu Kush region of central Asia, Ph.D. thesis, Mass. Inst. of Technol., Cambridge, 1981.

Shanov, S., E. Spassov, and T. Georgiev, Evidence for the existence of a paleosubduction zone beneath the Rhodopean massif (Central Balkans), *Tectonophysics, 206*, 307-314, 1992.

Spakman, W., Subduction beneath Eurasia in connection with the Mesozoic Tethys, *Geol. Mijnbouw., 65*, 145-153, 1986.

Spakman, W., Upper mantle delay time tomography with an application to the collision zone of the Eurasian, African and Arabian plates, Ph.D. thesis, 200 pp., Univ. of Utrecht, Utrecht, Netherlands, 1988.

Spakman, W., M. J. R. Wortel, and N. J. Vlaar, The Hellenic subduction zone: A tomographic image and its dynamic implications, *Geophys. Res. Lett., 15*, 60-63, 1988.

Spakman, W., S. Van der Lee, and R. D. Van der Hilst, Travel-time tomography of the European-Mediterranean mantle down to 1400Km, *Phys. Earth Planet. Inter., 79*, 3-74, 1993.

Thurber, C. H., and W. L. Ellsworth, Rapid solution of ray tracing problems in heterogeneous media, *Bull. Seismol. Soc. Am., 70*, 1137-1148, 1980.

Vogt, P., and P. Higgs, An aeromagnetic survey of the eastern Mediterranean sea and its interpretation, *Earth. Planet. Sci. Lett., 5*, 439-448, 1969.

Voulgaris, N., Investigation of the crustal structure in western Greece (Zakinthos - NW Peloponessus area) (in Greek), Ph.D. Thesis, Univ. of Athens, Athens, Greece, 1991.

Wortel, M. J. R., S. B. D. Goes, and W. Spakman, Structure and seismicity of the Aegean subduction zone, *Terra Nova, 2*, 554-562, 1990.

P. M. Hatzidimitriou, D.G. Panagiotopoulos, C. B. Papazachos, and G. N. Tsokas, Geophysical Laboratory, Aristotle University of Thessaloniki, Thessaloniki, Greece, GR-54006. (e-mail: kpapazachos@olymp.ccf.auth.gr)

(Received April 7, 1994; revised January 30, 1995; accepted February 23, 1995.)